Astron. Astrophys. 350, 635–642 (1999)

ASTRONOMY AND ASTROPHYSICS

The Wilson-Bappu relation for RS CVn stars

F.F. Özeren[1,2], **J.G. Doyle**[1], **and D. Jevremovic**[1,3]

[1] Armagh Observatory, College Hill, Armagh BT61 9DG, Ireland (jgd@star.arm.ac.uk)
[2] Department of Astronomy, Science Faculty of Ankara University, 06100 Tandoğan-Ankara, Turkey (ferhat@astro1.science.ankara.edu.tr)
[3] Belgrade Observatory, Volgina 7, 11050 Belgrade, Yugoslavia (darko@aob.aob.bg.ac.yu)

Received 12 May 1999 / Accepted 27 August 1999

Abstract. We investigate the extent to which the Wilson-Bappu relationship holds for chromospherically active binaries using the Mg II h&k lines of 41 RS CVn stars observed with IUE. The resulting fits are different from the relationships obtained for single, less active stars. The parallax used were those from the HIPPARCOS catalogue, these give a much better correlation than the magnitudes taken from CABS. Within a particular luminosity class the relationship is good, however it tends to break down when we incorporate objects ranging in luminosity from class I to V. From model calculations there is very little dependence of the Mg II line width on effective temperature. The line width does however depend on the column mass at the transition region boundary showing increased line width at lower column mass. There is also a dependence on the column mass adopted for the temperature minimum, however, the major and dominant parameter is the surface gravity scaling as $g^{-1/4}$. Within a luminosity class more active objects will show larger lines widths reflecting a higher column mass deeper in the atmosphere, e.g. at the temperature minimum level.

Key words: line: formation – stars: activity – stars: chromospheres – stars: late-type

1. Introduction

The Wilson-Bappu relationship (hereafter the WB relationship) was first established as a relation between the absolute visual magnitude (M_v) and the line width of Ca II H&K emission lines for late type stars by Wilson & Bappu (1957). Subsequent work, based on COPERNICUS data for a very limited sample of K giants (McClintock et al. 1975) extended it to other lines, notably Mg II h&k and Ly α. Many other authors, (e.g. Kondo et al. 1976; Stencel 1977; Weiler & Oegerle, 1979; Vladilo et al., 1987, Montes et al. 1994) have looked at the WB relationship attempting to explain the under-laying physics.

There are two plausible basic theories to explain the WB relationship i) Doppler broadening with stellar absolute magnitude ii) column density above the temperature minimum. These were discussed in papers by Engvold & Rygh (1978), Ayres (1979), Linsky (1980) and Lutz & Pagel (1982). The dominant parameter seems to be the chromospheric mass column density.

To extend and test the WB relationship for low luminosity objects, the red dwarf stars AU Mic, AT Mic and AD Leo were used (Elgarøy, 1988, Ambruster et al., 1989). These new data points fitted well with the result of Vladilo et al. (1987). Going to the more active stars, Gurzadyan (1991) used 10 RS CVn-type objects. He concluded that the observed magnesium emission was generated by ionized gas in the space between the components of the binary systems. Montes et al. (1994) used Ca II H&K for 28 chromospherically active binary systems and 18 single active stars. They noted that there is a systematic difference among the behaviour of stars belonging to different groups. Elgarøy et al. (1997), working with Mg II h&k data for 78 single stars observed with IUE noted that the active stars show a somewhat larger spread in line widths than the 'quieter' objects, thus showing a different WB relation. Recently, a re-calibration of the WD relationship has been done for 94 stars with absolute magnitudes derived from the parallax's reported from HIPPARCOS (Scoville & Mena-Werth, 1998)

Due to the prolific output from IUE during it's 19 years of operation, an excellent dataset of Mg II h&k line profiles has been obtained for a large selection of RS CVn binaries. With the exception of the latter few references, most of the developed WB relationships have excluded RS CVn's, due to their intense chromospherically activity and binary nature. Here, we look again at the WB relationship, confining ourselves only to the RS CVn's using the absolute magnitudes based on the new HIPPARCOS parallax's. The parallax parameter along gives substantially different results than those based on Strassmeier et al. (1993) catalogue. In the final section of the paper we compare the result from the observational data with Mg II k line profiles as calculated with MULTI for a range of gravities, effective temperatures, column mass in the transition region and column mass at the temperature minimum.

2. Observational data and its reduction

We have searched the IUE Data Archive for the entire CABS (Strassmeier et al. 1993). Mostly only LWP data was reduced, although sometimes data from the LWR camera was also used. Related parameters are given in Tables 1 & 2, e.g. the CABS

Send offprint requests to: Ferhat Fikri Özeren

Table 1. The individual parameters for the stars in the sample.

NO	CABS	HIP	Star Name	HD	Sp	$P_{\rm orb}$(day)	$P_{\rm rot}$(day)	Log g	T_{eff}
1	3	664	AP Psc	352	$\sim$ F/K1III	96.439		-/2.78	4106[2]
2	5	2762	13 Cet	3196	F7/G4	2.082		-/4.46	5708[2]
3	7	3693	ζ And	4502	/K1III	17.7692		-/2.78	4481[1]
4	8	4157	CF Tuc	5303	G0V/K4IV	2.79786	2.798	4.39/3.37	4452[2]
5	9	5007		6286	G2V	91.9		4.40	
6	10	5951	AY Cet	7672	WD/G5III	56.824	77.22	-/3.07	-/4930[1]
7	16	9630		12545	K0III	23.9824	24.3	2.89	
8	22	13118	VY Ari	17433	K3-4 V-IV	13.198	16.42	4.50	
9	29	16846	V711 Tau	22468	G5IV/K1IV	2.83774	2.841	3.71/3.55	4912[2]
10	48	23743	BM Cam	32357	K0III	80.895	85	2.89	4510[1]
11	71		YY Gem		dM1e/dM1e	0.8142822	0.8143	4.67/4.67	
12	81	44134	TY Pyx	77137	G5IV/G5IV	3.198584	3.32	3.71/3.71	5436[2]
13	85	46159	IL Hya	81410	K1III	12.908	12.89	2.78	4650[2]
14	96	56862	GT Mus	101379	A0/K2-4III	61.36	56.03	-/2.36	9520/4808[1]
15	112	65187	BM CVn	116204	K1III	20.625	20.6	2.78	4424[1]
16	116	67013	V851 Cen	119285	K2IV-III	11.989	12.05	2.63	4311[1]
17	118		V841 Cen	127535	K1IV	5.998	5.929	3.55	4389[1]
18	120	72848		131511	K2V	125.369		4.55	
19	125		UZ Lib		$\sim$ A8/K0III	4.767885	4.7357	-/2.89	
20	132	79607	TZ CrB	146361	F6V/G0V	1.139791	1.1687	4.30/4.39	6352/5948[2]
21	136	81519	WW Dra	150708	G2IV/K0IV	4.629617	4.62961	3.77/3.57	4650[2]
22	137	82080	ϵ UMi	153751	A8-F0V/G5III	39.4809		4.28/3.07	7370/5011[1]
23	141	84586	V824 Ara	155555	G5IV/K0V-IV	1.681652	1.682	3.71/3.57	5048[2]
24	144	85852	DR Dra	160538	WD/K0-2III	905.9	31.05	-/2.78	-/4602[1]
25	147	87965	Z Her	163930	F4V-IV/K0IV	3.992801	3.962	3.98/3.57	5048[2]
26	152	88848	V815 Her	166181	G5V/M1-2V	1.809837	1.819	4.49/-	5542[2]
27	156	91009	BY Dra	234677	K4V/K7.5V	5.975112	3.827	4.57/4.62	
28	159	92512	o Dra	175306	G9III	138.42	142.8	2.92	4291[1]
29	163	94013	V1762 Cyg	179094	K1IV-III	28.5895	28.5895	2.78	4569[1]
30	165	95244	V4138 Sgr	181809	K1III	13.048	60.23	2.78	4613[1]
31	167	96003	V1817 Cyg	184398	A2V/K2III-II	108.854	108.854	4.16/2.63	8970[1]
32	179	103833	ER Vul	200391	G0V/G5V	0.698095	0.6942	4.49/4.49	5948/5678[2]
33	187	107095	42 Cap	206301	G2IV	13.174		3.77	5738[2]
34	190	109002	HK Lac	209813	F1V/K0III	24.4284	24.461	4.27/2.89	4692[2]
35	191	109303	AR Lac	210334	G2IV/K0IV	1.98	1.98	3.77/3.57	5616/5048[2]
36	194	111072	V350 Lac	213389	K2III	17.755		2.63	4393[1]
37	195	111802	FK Aqr	214479	dM2e/dM3e	4.08322	4.39	4.69/4.71	
38	196	112997	IM Peg	216489	K2III-II	24.65	24.39	2.63	4534[1]
39	202	114639	SZ Psc	219113	F8IV/K1IV	3.965866	3.955	3.89/3.55	6500/5500[1]
40	204	116584	λ And	222107	G8IV-III	20.5212	53.952	2.89	4842[2]
41	206	117915	II Peg	224085	K2-3 V-IV	6.724183	6.718	3.20	4842[2]

Notes: [1] Barrado y Navascues, D. et al. (1998), [2] Gunn, A. et al. (1998)

number, HIPPARCOS number, Star Name, HD number, spectral type, V-band magnitude, (B–V) color, $P_{\rm (orb)}$, $P_{\rm (rot)}$, log g, T_{eff}, π in milli arc second from HIPPARCOS, d in pc, absolute magnitudes and radius.

In Table 2, M_v is calculated by

$$M_v = V - 5logd(pc) + 5 - A_v \quad (1)$$

where $A_{\rm v}$ is the correction for interstellar absorption expressed in V magnitude. The corrections were obtained using

$$A_v = 3.2 * E(B-V) \quad (2)$$

$$E(B-V) = (B-V)_{\rm observed} - (B-V)_{\rm intrinsic} \quad (3)$$

The intrinsic (B–V) colours were taken from Fitzgerald (1970). For conversion to surface flux, the radius was taken from CABS, Gunn et al. (1998) or Straižys & Kuriliene (1981).

To analyse the IUE images we used the STARLINK package DIPSO (Howarth et al. 1996). The widths and the emission line fluxes of the Mg II h&k lines were measured using a least squares Gaussian fit (Table 3). Some stars have more than one spectra, in this situation the resultant values are given as a mean value in Table 3. All derived line widths are corrected for the instrumental broadening using a square correction

$$W^2 = W^2_{\rm observed} - W^2_{\rm instrumental} \quad (4)$$

Table 2. The individual parameters for the stars in the sample (see text for description).

NO	Star Name	V_{CABS}	V_{HIP}	$(B-V)_{CABS}$	$(B-V)_{HIP}$	$\pi(mars)_{HIP}$	d(pc)	M_v	$M_{v_{HIP}}$	R^{ref}
1	AP Psc	6.07	6.32	1.38	1.366	3.25	307.69	-0.1	-2.00	41[1]
2	13 Cet	5.2	5.32	0.57	0.567	47.51	21.05	3.9/	4.00	1.3[2]
3	ζ And	4.06	4.25	1.12	1.100	17.98	55.62	1.9	0.49	0.7[1]
4	CF Tuc	7.41	7.74	0.735	1.561	3.51	284.9	[4.4/3.1:]	-2.32	3.32[2]
5	HD6286	8.4	8.36	[0.63]	0.960	4.64	215.52	[4.7]	0.64	1.02[3]
6	AY Cet	5.47	5.58	0.9	0.888	16.08	62.19	/1.32	1.14	15[1]
7	HD12545	8.11	8.56	1.21	1.107	5.08	196.08	/0.13	1.78	8[1]
8	VY Ari	6.9	7.08	0.96	0.956	22.73	44.0	5.2	3.91	0.76[3]
9	V711 Tau	5.7	6.04/8.90	0.92	0.885	34.52	28.97	4.2/3.2	3.13/6.93	1.3/3.9[1]
10	BM Cam	6.1	6.24	1.12	1.112	5.22	191.57	0.2	-0.49	16[1]
11	YY Gem	9.07	-.–	1.35	-.—	-.–	—.–	9.14		0.62[1]/0.54[3]
12	TY Pyx	6.835	7.02	0.72/0.76	0.695	17.91	55.83	3.9/3.8	3.30/3.30	1.59/1.68[1]
13	IL Hya	7.25	7.52	1.02	1.012	8.36	119.62	0.15	2.38	12[2]
14	GT Mus	5.08	5.18	0.79	0.804	5.81	172.41	0.3	-0.14	16.6[3]
15	BM CVn	7.21	7.48	1.16	1.157	9.00	111.11	0.2	2.03	16[2]
16	V851 Cen	7.81	7.78	1.067	1.068	13.13	76.16	3.5	3.67	3.5[1]
17	V841 Cen	8.5	-.–	1.069	-.—	–.–	–.–	4.6	3.12	3.16[3]
18	HD131511	5.97	6.14	0.84	0.841	86.69	11.54	6.1	6.09	0.78[3]
19	UZ Lib	9.3	-.–	1.06	-.—	–.–	–.–	[/0.7]	-.–	21[1]
20	TZ CrB	5.7	5.71/6.74	0.47	0.599	46.11	21.69	4.1	3.65/5.06	1.22/1.21[1]
21	WW Dra	8.22	8.75/9.71	0.6	0.714	8.67	115.3	3	3.07/4.87	2.12/3.9[2]
22	ϵ UMi	4.23	4.37	0.89	0.897	9.41	106.27	0	-2.67/-0.75	1.7/12[1]
23	V824 Ara	6.63	7.01	0.835	0.798	31.83	31.42	4/5.2	4.21/4.72	1.61/1.25[2]
24	DR Dra	6.55	6.77	1.05	1.043	9.68	103.31	-0.1	1.86	10[3]
25	Z Her	7.23	7.37	0.59	0.602	10.17	98.33	2.9/3.5	1.76/3.39	1.85/2.73[1]
26	V815 Her	7.66	7.83	0.72	0.728	30.69	32.6	5.2	7.64	0.97[2]
27	BY Dra	8.07	8.28	1.221	1.265	60.90	16.42	7.6/8.6	6.36/7.48	0.7/0.6[3]
28	o Dra	4.64	4.79	1.19	1.185	10.12	98.81	0.5	-0.84	14.3[2]
29	V1762 Cyg	5.81	6.05	1.09	1.086	14.24	70.22	1.67	1.83	9.2[2]
30	V4138 Sgr	6.57	6.89	1.03	1.032	11.40	87.72	0.15	2.36	11.22[3]
31	V1817 Cyg	6.32	6.52	1.16	1.123	3.10	322.58	-1.1	-1.15	62[1]
32	ER Vul	7.27	7.46	[0.95]	0.614	20.06	49.85	4.62/4.74	3.93/4.18	1.07/1.07[1]
33	42 Cap	5.17	5.29	0.65	0.672	30.73	32.5	3	2.50	3[2]
34	HK Lac	6.52	7.09	1.08	1.052	6.62	151.06	3/0.8	1.06	15[2]
35	AR Lac	6.09	6.25	0.72	0.763	23.79	42.0	3.5/3.3	2.74/3.13	1.52/2.72[2]
36	V350 Lac	6.38	6.57	1.17	1.166	8.18	122.25	2.2	1.12	12.7[2]
37	FK Aqr	9.05	9.13	1.5	1.466	115.71	8.6	9.5	9.46	0.5/0.44[3]
38	IM Peg	5.6	6.03	1.12	1.132	10.33	96.81	2.0	1.10	7[2]
39	SZ Psc	7.2	7.55	0.44/1.00	0.788	11.34	88.2	3.3/2.3	3.28	5.1[2]
40	λ And	3.7	3.97	1.01	0.984	38.74	25.81	2.2	1.61	7[2]
41	II Peg	7.51	7.61	1.01	1.007	23.62	42.3	5.4	4.96	2.2[2]

Notes: [1] Strassmeier et al. (1993), [2] Gunn et al. (1998), [3] Straizy & Kuriliene (1981)

where $W_{\rm instrumental} = 21\ km\ s^{-1}$ (Turnrose & Thomson 1984). In Table 3, the FWHM of the Mg II h&k lines, $logW_{\rm h}$, $logW_{\rm k}$ and the fluxes for each line are presented.

3. Observational results

In Fig. 1 we plot $P_{\rm orb}$ versus the $P_{\rm rot}$. With the exception of a few objects, there is a strong correlation between them ($r = 0.95$) implying tidally locked systems. From Table 3 we note that the surface fluxes are higher than log $F_{\rm surface,k} = 5.2$ which was given as an activity measurement by Elgarøy et al., (1997). Fig. 2 shows the $M_{\rm v}$ - log W (km s^{-1}) relation of Mg II k for our sample of RS CVn's. In this figure, we have also plotted the points for the active and quiet stars as given by Elgarøy (1997) for Mg II k. The Mg II k least squares fit for all the objects in Fig. 2 is

$$M_{\rm v} = -15.50(\pm0.67) log\ W_{\rm MgIIk} + 32.45(\pm1.28) \quad (5)$$

with a correlation coefficient of r=0.82, while that for only the RS CVn's is

$$M_{\rm v} = -12.01(\pm0.89) log\ W_{\rm MgIIk} + 26.41(\pm1.82) \quad (6)$$

with a correlation coefficient of r=0.80. This relation is somewhat different from the relation for single stars with the RS CV

Table 3. Spectroscopic results for the RS CVn stars in the sample.

NO	Star Name	$FWHM_h$ (Å)	$\pm\sigma$	$\log W_h$ ($km\ s^{-1}$)	$\pm\sigma$	$\log F_h$	$FWHM_k$ (Å)	$\pm\sigma$	$\log W_k$ ($km\ s^{-1}$)	$\pm\sigma$	$\log F_k$
1	AP Psc	1.639	0.112	2.244	0.029	5.919	1.716	0.045	2.265	0.011	6.077
2	13 Cet	0.490	0.205	1.720	0.169	6.468	0.611	0.072	1.817	0.049	6.466
3	ζ And	1.253	0.008	2.128	0.003	8.713	1.399	0.012	2.177	0.004	8.863
4	CF Tuc	1.282	0.279	2.137	0.094	7.524	1.655	0.055	2.249	0.014	7.607
5	HD6286	1.274	0.121	2.135	0.041	8.251	1.616	0.050	2.239	0.013	8.339
6	AY Cet	0.799	0.111	1.932	0.059	5.665	0.930	0.035	1.999	0.016	5.785
7	HD12545	1.105	0.188	2.073	0.073	6.663	1.092	0.077	2.069	0.030	6.663
8	VY Ari	0.704	0.057	1.877	0.034	7.571	0.756	0.033	1.909	0.019	7.622
9	V711 Tau[1]	0.882		1.975		6.889	0.982		1.975		7.055
10	BM Cam	1.219	0.041	2.116	0.014	6.553	1.662	0.026	2.251	0.007	6.648
11	YY Gem (Pri.)	0.639	0.012	1.835	0.008		0.617	0.017	1.821	0.011	
	YY Gem (Sec.)	0.368	0.011	1.596	0.012		0.565	0.017	1.782	0.013	
12	TY Pyx[2] (Pri.)						0.860	0.060	1.965	0.030	6.921
	TY Pyx[2] (Sec.)						0.850	0.030	1.959	0.015	6.869
13	IL Hya	0.891	0.047	1.979	0.022	5.890	1.022	0.027	2.040	0.011	5.953
14	GT Mus	1.512	0.196	2.209	0.056	6.793	1.802	0.106	2.286	0.026	6.896
15	BM CVn	1.076	0.059	2.062	0.023	5.606	1.057	0.024	2.055	0.010	5.730
16	V851 Cen	0.769	0.012	1.915	0.007	6.575	0.780	0.011	1.923	0.006	6.749
17	V841 Cen	0.883	0.051	1.975	0.025	6.258	1.088	0.033	2.067	0.013	6.250
18	HD131511	0.513	0.027	1.740	0.021	6.261	0.541	0.020	1.764	0.015	6.310
19	UZ Lib	1.190	0.141	2.105	0.051		1.850	0.133	2.298	0.031	
20	TZ CrB (Pri.)	0.551	0.065	1.771	0.048	6.480	0.699	0.031	1.875	0.018	6.593
	TZ CrB (Sec.)	0.568	0.071	1.784	0.051	6.452	0.761	0.032	1.912	0.018	6.563
21	WW Dra(Pri.)	1.084	0.206	2.065	0.081	6.061	1.293	0.191	2.261	0.063	6.214
	WW Dra (Sec.)	0.807	0.084	1.936	0.044	5.793	0.931	0.066	2.080	0.030	5.933
22	ϵ UMi	1.173	0.076	2.099	0.028	6.452	1.373	0.047	2.168	0.015	6.580
23	V824 Ara(Pri.)	0.537	0.018	1.760	0.013	6.236	0.689	0.014	1.869	0.008	6.357
	V824 Ara(Sec.)	0.516	0.022	1.742	0.017	6.320	0.595	0.018	1.805	0.013	6.389
24	DR Dra	0.815	0.063	1.941	0.033	6.084	0.955	0.025	2.011	0.011	6.118
25	Z Her	0.811	0.109	1.938	0.057	6.484	0.865	0.039	1.968	0.019	6.569
26	V815 Her	0.535	0.016	1.758	0.012	6.449	0.670	0.030	1.857	0.019	6.605
27	BY Dra (Pri.)	0.303	0.035	1.511	0.043	6.077	0.326	0.017	1.544	0.019	6.157
	BY Dra (Sec.)	0.245	0.046	1.419	0.064	6.049	0.310	0.022	1.521	0.026	6.159
28	o Dra	1.170	0.196	2.098	0.072	5.894	1.131	0.105	2.084	0.040	6.068
29	V1762 Cyg	0.992	0.098	2.026	0.042	6.184	1.180	0.050	2.103	0.018	6.286
30	V4138 Sgr	0.807	0.038	1.936	0.020	5.840	0.823	0.019	1.946	0.010	5.912
31	V1817 Cyg	1.866	0.311	2.301	0.072	5.613	1.950	0.131	2.321	0.029	5.763
32	ER Vul(Pri.)	1.358	0.329	2.162	0.104	6.688	1.396	0.092	2.176	0.028	6.775
	ER Vul(Sec.)	1.368	0.322	2.166	0.101	6.689	1.483	0.118	2.202	0.034	6.803
33	42 Cap	0.604	0.037	1.810	0.025	5.999	0.644	0.044	1.840	0.028	6.184
34	HK Lac	1.306	0.044	2.145	0.014	6.199	1.404	0.048	2.178	0.015	6.271
35	AR Lac (Pri.)	1.084	0.067	2.065	0.027	6.824	1.295	0.036	2.143	0.012	6.972
	AR Lac (Sec.)	0.752	0.078	1.906	0.044	5.981	0.965	0.053	2.015	0.023	6.086
36	V350 Lac	1.347	0.148	2.159	0.047	6.128	1.521	0.071	2.213	0.020	6.201
37	FK Aqr (Pri.)	0.153	0.015	1.214	0.027	5.416	0.203	0.016	1.338	0.025	5.609
	FK Aqr (Sec.)	0.241	0.011	1.412	0.016	5.826	0.302	0.014	1.511	0.017	5.963
38	IM Peg[3]	1.305		2.145		6.810	1.464		2.196		6.922
39	SZ Psc	1.658	0.058	2.249	0.015	6.360	1.842	0.047	2.296	0.011	6.466
40	λ And	0.838	0.056	1.953	0.028	6.367	0.974	0.005	2.019	0.002	6.459
41	II Peg	0.697	0.015	1.873	0.009	6.599	0.827	0.004	1.948	0.002	6.647

Notes: [1] Dempsey et al. (1996), [2] Neff et al. (1996), [3] Oláh et al. (1998)

objects showing a larger variation in the line width. It is however clear that stars ranging from luminosity I to luminosity V can have a similar line width but differing in absolute magnitude by a factor of seven. This therefore reflects the growing importance of the radius and effective temperature in the super-giants and giants, suggesting that $log\,W$ versus M_V are not the best param-

Table 4. Parameters used in the modelling: effective temperature (T_{eff}), surface gravity ($log\, g$) in $cm\, s^{-2}$, position of the transition region ($log\, m_{TR}$) in $g\, cm^{-2}$ and position of the temperature minimum ($log\, m_{min}$) in $g\, cm^{-2}$. All possible combinations of parameters were explored.

T_{eff}	$log\, g$	$log\, m_{TR}$	$log\, m_{min}$
3750, 4000, 4500, 5000	4.5, 4.0, 3.5, 3.0, 2.5	–4.5, –4.0, –3.5, –3.0, –2.9, –2.8, –2.7	–1.0, –0.5, 0.0

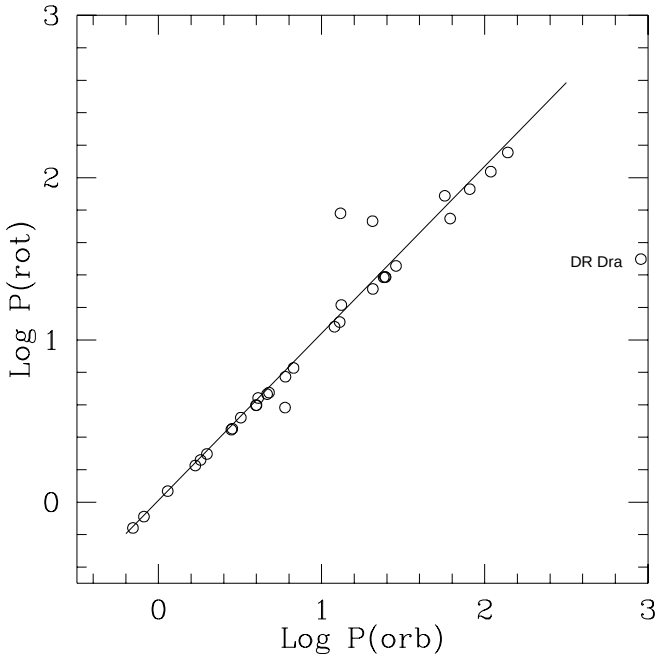

Fig. 1. logP_{rot} versus logP_{orb} for the stars in Table 1.

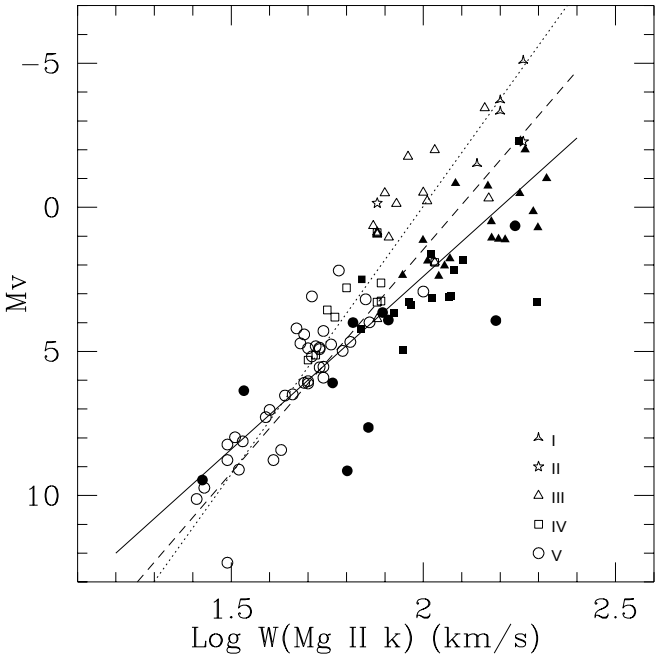

Fig. 2. The Wilson-Bappu relation for the Mg II k line. The solid line only shows our relation for the RS CVn's only, the dashed line shows the relation for all objects. Active & quiet single stars (un-filled symbols), RS CVn's (filled symbols), while the dotted line shows the relation for only the active and quiet single stars.

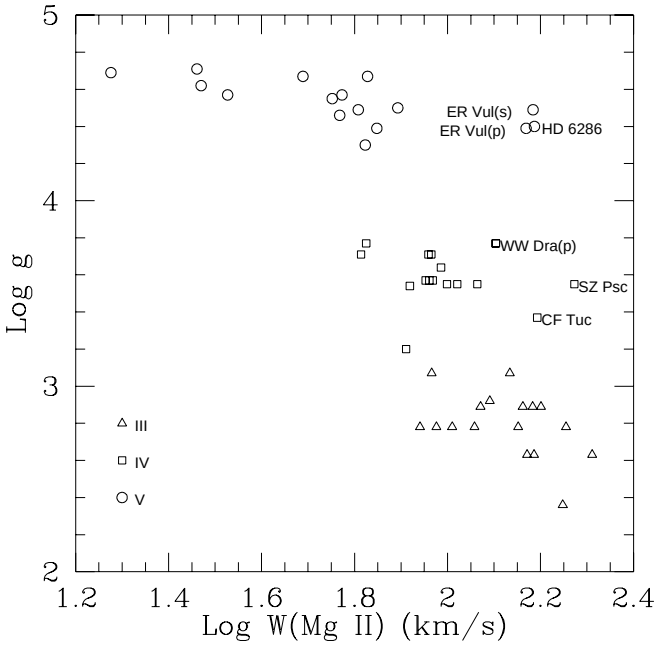

Fig. 3. Surface gravity versus log W (km s^{-1}) for the group of RS CVn stars.

eters to attempt a correlation if objects of differing luminosity classes are involved.

Fig. 3 shows the surface gravity versus log W(km s^{-1}). It is immediately clear that a very good correlation exists although there are exceptions which are probably due to the method of deriving $log\, g$. The present values were derived by using the spectral type as given by Straižys & Kuriliene (1981). This figure shows that different luminosity classes have different line widths with the higher luminosity objects showing broader lines (see also discussion by Lutz & Pagel 1982, Neckel 1974 and Reimers 1973). In an attempt to understand the various parameters involved in the formation of Mg II, we constructed (see Sect. 4) a series of model atmospheres varying T_{eff}, $log\, g$, the column mass at the temperature minimum and the column mass at the transition region.

4. Atmospheric models

We have calculated a grid of models representing the active component of RS CVn stars in order to investigate in more detail the dependence of the Mg II k line width on effective temperature (varied between 3750 and 5000 K), stellar surface gravity (between $log\, g = 2.5$ and 4.5), position of the temperature minimum ($log\, m_{min}$ from –1 to 0) and position of the transition region ($log\, m_{TR}$=–4.5 to –2.7). We adopted this particular range of values to cover both the active and very active stars as

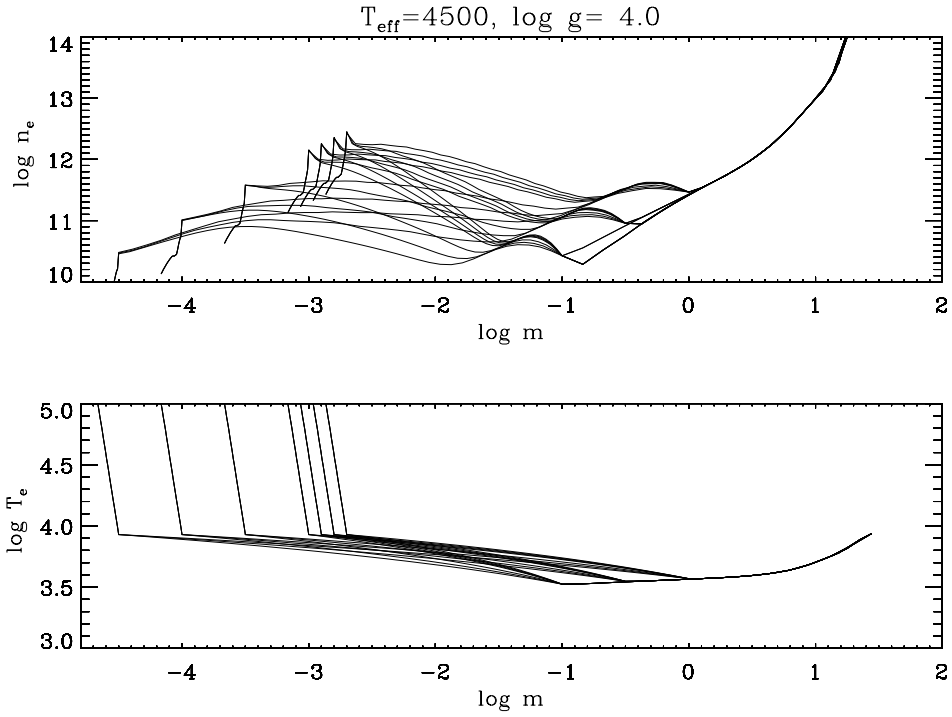

Fig. 4. The adopted atmospheric structures - electron densities (upper panel) and electron temperatures (lower panel) vs. column mass for an effective temperature of 4500K and $log\, g\, =\, 4$.

Short et al. (1998) have shown that the transition region in the RS CVn system II Peg is at a very deep position (-2.8).

A total of 420 atmospheric structures were calculated with the photospheric models of Kurucz (1992). Following Ayres (1979), all models have $T(m_{\rm TR})$ equal to ≈ 8500 K, the temperature at the top of the chromosphere. Because the atmosphere below $T_{\rm min}$ is close to radiative equilibrium (RE), the choice of $T_{\rm min}$ fixes the value of $m_{\rm min}$. We assume that the atmosphere is in radiative equilibrium up to the temperature minimum. With the chosen position of the temperature minimum and the position of the transition region we then built a series of simple models by keeping $\frac{dT}{dlogm}$ constant in the chromosphere (e.g. Short et al. 1998, Short & Doyle 1997). The grid of typical atmospheric structures (temperature and electron density distribution) for T_{eff} of 4500K and $log\, g\, =\, 4.0$ are shown in Fig 4, further details are given in Table 4.

With this range of parameters, we solve the hydrostatic equilibrium equation and NLTE problem for Hydrogen using the radiative transfer code MULTI version 2.2 (Carlsson 1986). This solution gives us the populations levels for Hydrogen and the correct distribution of electron densities in the structures. After that we solve the NLTE problem for the Mg II atom using a model atom with 18 levels. We converge the population levels of Mg II until changes are less than 1%.

Short & Doyle (1997) and Andretta et al. (1996) have shown that for models of cooler stars it is necessary to incorporate a better treatment for background opacities. We did not follow their treatment of background opacities mainly because of the huge computational requirements for our number of models. However, since we deal with larger effective temperatures than that considered by the above authors, this effect should not be major (less than 0.1 dex. in width).

5. Discussion

In Fig. 5 we show four plots of the dependence of the FWHM of the Mg II k line on stellar gravity and position for the transition region for different effective temperatures. For each position of the transition region, three values are plotted corresponding to different positions of the temperature minimum. The gravity dependence is clearly visible, however the dependence on effective temperature is small as seen by the similarity of the plots. In summary the calculations show that (i) for a higher transition region column mass the line width is smaller scaling as $m_{TR}^{-1/4}$, (ii) with increased effective temperature there is a greater dependence of the line width on the column mass at the temperature minimum, (iii) with increasing column mass at the temperature minimum there is an increase in line width scaling as $m_{min}^{0.1}$ and (iv) increasing line width as the surface gravity decreases scaling as $g^{-1/4}$.

In his analysis, Ayres (1979) gave a qualitative description of the dependence of the FWHM of the resonance lines of single ionized Magnesium and Calcium. For Mg II k the base line width was given by

$$\Delta\lambda_* \sim \tilde{\mathcal{F}}^{1/4}\tilde{g}^{-1/4}\tilde{T}_{eff}^{7/4} \tag{7}$$

and thermalization width by

$$\Delta\lambda_\Lambda \sim \tilde{\mathcal{F}}^{-1/4}\tilde{g}^{-1/4}\tilde{T}_{eff}^{-5/4}\xi^{1/2} \tag{8}$$

where $\tilde{\mathcal{F}}$, $\tilde{g}$ and $\tilde{T}_{eff}$ are the chromospheric heating, surface gravity and effective temperature expressed in solar units and ξ is the chromospheric Doppler width. Both of these widths have the same gravity dependence but opposite sensitivity on chromospheric heating. For the thermalization width there is only a weak dependence on the chromospheric velocity fields.

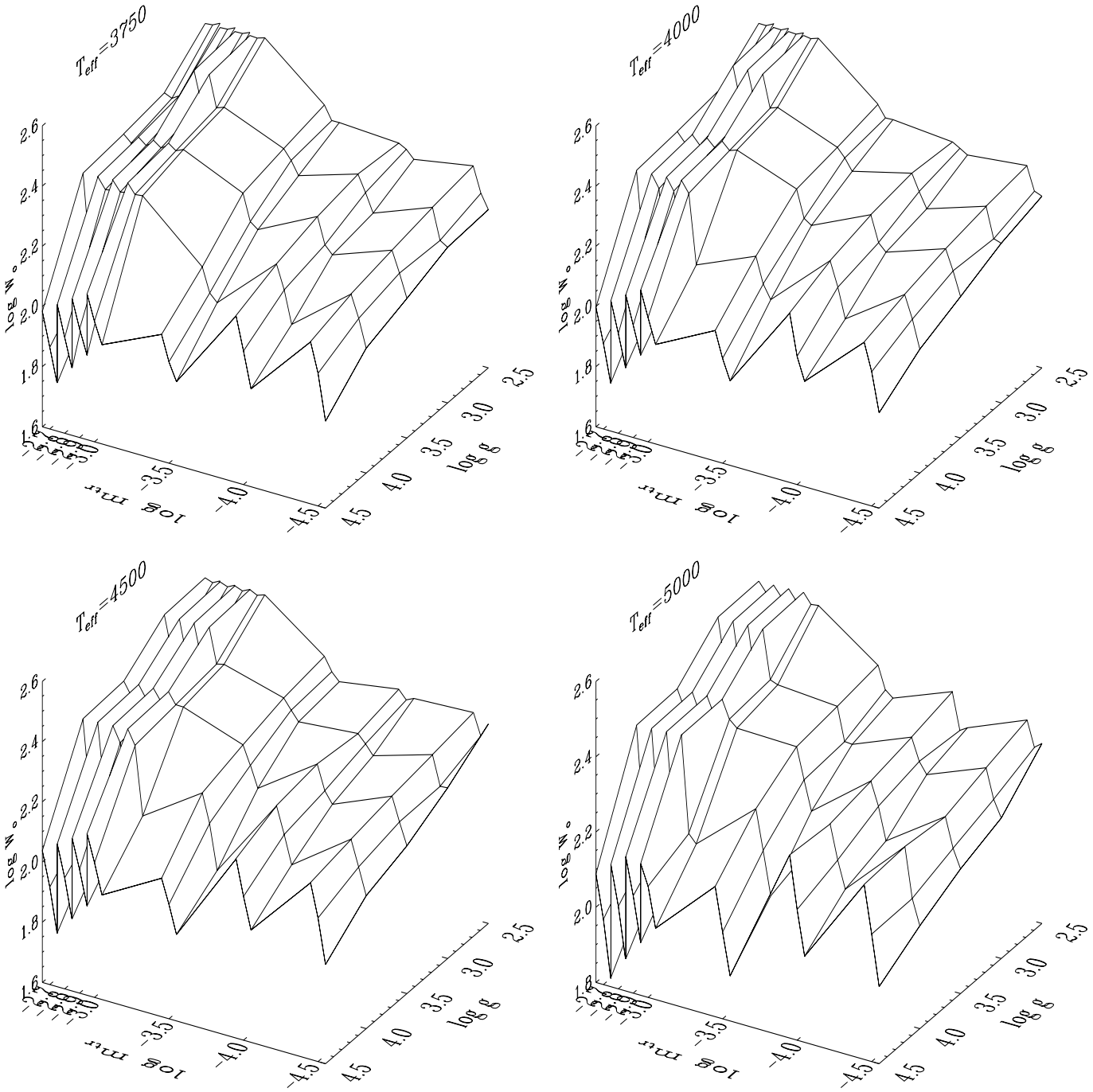

Fig. 5. Full width at half maximum ($log\, W$) of the Mg II k line versus $log\, g$ and $log\, m_{TR}$ for four different effective temperatures. Note that for each $log\, m_{TR}$, we have three separate lines for the column mass ($log\, m_{min}$) at T_{min}.

This suggested that log W is mainly sensitive to surface gravity ($W \sim g^{-1/4}$) but insensitive to effective temperature and heating. This is also clear from our calculations and also from the empirical data analysed. Also from Fig. 5 it is clear that there exist a qualitative dependence of width on position of the temperature minimum - i.e. a deeper temperature minimum generally gives wider lines.

Acknowledgements. Research at Armagh Observatory is grant aided by DENI while support for software and hardware is largely provided by the STARLINK Project which is funded by the UK PPARC. FFÖ wished to thank the Turkish Scientific and Technical Research Council for a grant which enabled a visit to Armagh. This work was supported in part by a grant (PPA/G/S/1997/00298) from the UK PPARC.

References

Ayres T.R., 1979, ApJ 228, 509
Ambruster C.W., Pettersen B.R., Sundaland S.R., 1989, A&A 208, 198
Andretta V., Doyle J.G., Byrne P.B., 1997, A&A 322, 266

Barrado y Navascues D., De Castro E., Fernandez-Figuero M.J., Cornide M., Garcia Lopez R.J., 1998, A&A 337, 739-753
Carlsson M., 1986, Uppsala Observatory Internal Report no. 33
Dempsey R.C., Neff J.E., Thorpe M.J., et al., 1996, ApJ 470, 1172
Elgarøy Ø., 1988, A&A 204, 147
Elgarøy Ø., Engvold O., Jorås P., 1997, A&A 326, 165
Engvold O., Rygh B.O., 1978, A&A 70, 399
Fitzgerald M.P., 1970, A&A 4, 234
Gunn A.G., Mitrou C.K., Doyle J.G., 1998, MNRAS 296, 150G
Gurzadyan G.A., 1991, Ap&SS 179, 293
Howarth I.D., Murray J., Berry D.S., 1996, DIPSO - A Friendly spectrum Analysis Program. STARLINK User Note 50.19
Kondo Y., Morgan T.H., Modisette J.L., 1976, ApJ 207, 167
Kurucz R.L., 1992, Rev. Mex. Astron. Astrofis. 23, 45
Linsky J.L., 1980, ARA&A 18, 439
Lutz T.E., Pagel B.E.J., 1982, MNRAS 199, 1101
McClintock W., Henry R.C., Moos H.W., 1975, ApJ 202, 733
Montes D., Fernandez-Figueroa M.J., DeCastro E., Cornide M., 1994, A&A 285, 609
Neckel H., 1974, A&A 35, 99
Neff J.E., Pagano I., Rodono M., et al., 1996, A&A 310, 173
Oláh K., Marik D., Houdebine E.R., Dempsey R.C., Budding E., 1998, A&A 330, 559
Reimers D., 1973, A&A 24, 79
Scoville F., Mena-Werth J., 1998, PASP 110, 794
Short C.I., Doyle J.G., 1997, A&A 326, 287
Short C.I., Byrne P.B., Panagi P.M., 1998, A&A 338, 191
Stencel R.E., 1977, ApJ 215, 176
Strassmeier K.G., Hall D.S., Fekel F.C., Scheck M., 1993, A&AS 100, 173
Straižys V., Kuriliene G., 1981, Ap&SS 80, 353
Turnrose B.E., Thomson R.W., 1984, IUE Processing Information Manual Version 2.0, CSC/TM-84/6058
Vladilo G., Molaro P., Crivellari L., et al., 1987, A&A 185, 233
Weiler E.J., Oegerle W.R., 1979, ApJS 39, 537
Wilson O.C., Bappu M.K.V., 1957, ApJ 125, 661